Counterflow-induced decoupling in superfluid turbulence

Dmytro Khomenko, Victor S. L'vov, Anna Pomyalov, and Itamar Procaccia
Department of Chemical Physics, Weizmann Institute of Science, Rehovot 76100, Israel

(Received 25 October 2015; revised manuscript received 9 January 2016; published 26 January 2016)

In mechanically driven superfluid turbulence, the mean velocities of the normal- and superfluid components are known to coincide: $\boldsymbol{U}_{\rm n} = \boldsymbol{U}_{\rm s}$. Numerous laboratory, numerical, and analytical studies showed that under these conditions, the mutual friction between the normal- and superfluid velocity components also couples their fluctuations: $\boldsymbol{u}'_{\rm n}(\boldsymbol{r},t) \approx \boldsymbol{u}'_{\rm s}(\boldsymbol{r},t)$, almost at all scales. We show that this is not the case in thermally driven superfluid turbulence; here the counterflow velocity $\boldsymbol{U}_{\rm ns} \equiv \boldsymbol{U}_{\rm n} - \boldsymbol{U}_{\rm s} \neq 0$. We suggest a simple analytic model for the cross-correlation function $\langle \boldsymbol{u}'_{\rm n}(\boldsymbol{r},t) \cdot \boldsymbol{u}'_{\rm s}(\boldsymbol{r}',t)\rangle$ and its dependence on $U_{\rm ns}$. We demonstrate that $\boldsymbol{u}'_{\rm n}(\boldsymbol{r},t)$ and $\boldsymbol{u}'_{\rm s}(\boldsymbol{r},t)$ are decoupled almost in the entire range of separations $|\boldsymbol{r} - \boldsymbol{r}'|$ between the energy-containing scale and intervortex distance.

DOI: 10.1103/PhysRevB.93.014516

I. INTRODUCTION

Much of the thinking about turbulence in quantum fluids such as ^{4}He at low temperature is still influenced by the "two-fluid" model of Landau and Tisza. Within this model, the dynamics of the superfluid ^{4}He is described in terms of a viscous normal component and an inviscid superfluid component, each with its own density, $\rho_{\rm n}(T)$ and $\rho_{\rm s}(T)$, and its own velocity field, $\boldsymbol{u}_{\rm n}(\boldsymbol{r},t)$ and $\boldsymbol{u}_{\rm s}(\boldsymbol{r},t)$. Due to the quantum-mechanical restriction, the circulation around the superfluid vortices is quantized to integer values of $\kappa = h/m$, where h is the Plank constant and m is the mass of the ^{4}He atom. The quantization of circulation results in the appearance of a characteristic "quantum" length scale: the mean separation between vortex lines, ℓ, which is typically orders of magnitude smaller than the scale H of the largest (energy-containing) eddies [1,2].

Experimental evidence [3,4] indicates that superfluid turbulence at large scales $R \gg \ell$ is similar to classical turbulence if the mechanical forcing is similar. Examples are furnished by a towed grid [5] forcing or by a pressure drop in a channel [6,7]. The reason for the similarity is that the interaction of the normal-fluid component with the quantized-vortex tangle leads to a mutual friction force [1,2,8], "which couples together $\boldsymbol{u}_{\rm n}(\boldsymbol{r},t)$ and $\boldsymbol{u}_{\rm s}(\boldsymbol{r},t)$ so strongly that they move as one fluid" [9]. This strong-coupling effect was demonstrated analytically in Ref. [10] and was later confirmed by numerical simulations of the two-fluid model [11,12] over a wide temperature range ($1.44 < T < 2.157$ K, corresponding to the ratio of densities $\rho_{\rm n}/\rho_{\rm s}$ from 0.1 to 10). The simulations showed strong locking of normal- and superfluid velocities at large scales, over one decade of the inertial range. In particular, it was found that even if either the normal fluid or the superfluid is forced at large scale (the dominant one), both fluids get locked very efficiently. Only detailed numerical simulations (in the framework of so-called shell models of turbulence) with a very large inertial interval [13,14] showed minor decoupling of $\boldsymbol{u}_{\rm s}$ and $\boldsymbol{u}_{\rm n}$ at the viscous edge of the inertial interval, in agreement with the analytical result of Ref. [10].

A different situation is expected for thermally driven superfluid turbulence. This type of turbulence is generated by a heater located at the closed end of a channel which is open at the other end to a superfluid helium bath. In this case, the heat flux is carried away from the heater by the normal fluid alone with the mean velocity $\boldsymbol{U}_{\rm n}$, and, by conservation of mass, a superfluid current with the mean velocity $\boldsymbol{U}_{\rm s}$ arises in the opposite direction. This gives rise to a relative (counterflow) velocity,

$$\boldsymbol{U}_{\rm ns} \equiv \boldsymbol{U}_{\rm n} - \boldsymbol{U}_{\rm s}, \tag{1}$$

which is proportional to the applied heat flux. Invariably, this counterflow excites an accompanying tangle of vortex lines. In counterflow experiments, there is no mean mass flux and the mean velocities $\boldsymbol{U}_{\rm s}$ and $\boldsymbol{U}_{\rm n}$ of the superfluid and the normal-fluid components are related as follows: $\rho_{\rm n}\boldsymbol{U}_{\rm n} + \rho_{\rm s}\boldsymbol{U}_{\rm s} = 0$.

A situation very similar to counterflow appears in superflows. Here, superleaks (i.e., filters located at the channel end with submicron-sized holes permeable only to the inviscid superfluid component) allow a net flow of the superfluid component in the channel. Contrary to counterflows, now the normal component remains stationary on the average: $\boldsymbol{U}_{\rm n} = 0$. In both counterflows and superflows, the normal- and superfluid components are moving with different mean velocities and their relative velocity $U_{\rm ns} \neq 0$.

Clearly, in both cases, one expects properties of the normal- and superfluid velocity fluctuations different from that in the mechanically driven "coflow" turbulence, in which $U_{\rm n} = U_{\rm s}$ and $U_{\rm ns} = 0$. The simple reason for that is illustrated in Fig. 1, in which eddies of scales $R_1 < R_2 < R_3$ are shown at three successive moments of time, $t = -\tau, t = 0$, and $t = \tau$, for coflow [Figs. 1(a)–1(c)] and for counterflow [Figs. 1(d)–1(f)].

In the coflow, the quantized-vortex tangles (blue solid lines) are swept by the superfluid component with the mean velocity close to $\boldsymbol{U}_{\rm s}$ together with the normal-fluid eddies (red dashed lines), which are swept by the normal-fluid component with their mean velocity $\boldsymbol{U}_{\rm n}$. Since in the coflow $U_{\rm s} = U_{\rm n}$, all (normal- and superfluid eddies) are swept with the same velocity, and the entire eddy configuration is moving as a whole from the left, in Fig. 1(a), to the right, in Fig. 1(c), in the "laboratory" reference system, shown in all panels as a black frame. During their common motion, the mutual friction effectively couples the velocities and $\boldsymbol{u}_{\rm n}(\boldsymbol{r},t) = \boldsymbol{u}_{\rm s}(\boldsymbol{r},t)$. The situation is completely different in the counterflow, where the mean velocities have opposite directions and $U_{\rm ns} \neq 0$. We have chosen for concreteness $U_{\rm n} > 0$, and therefore the normal-fluid

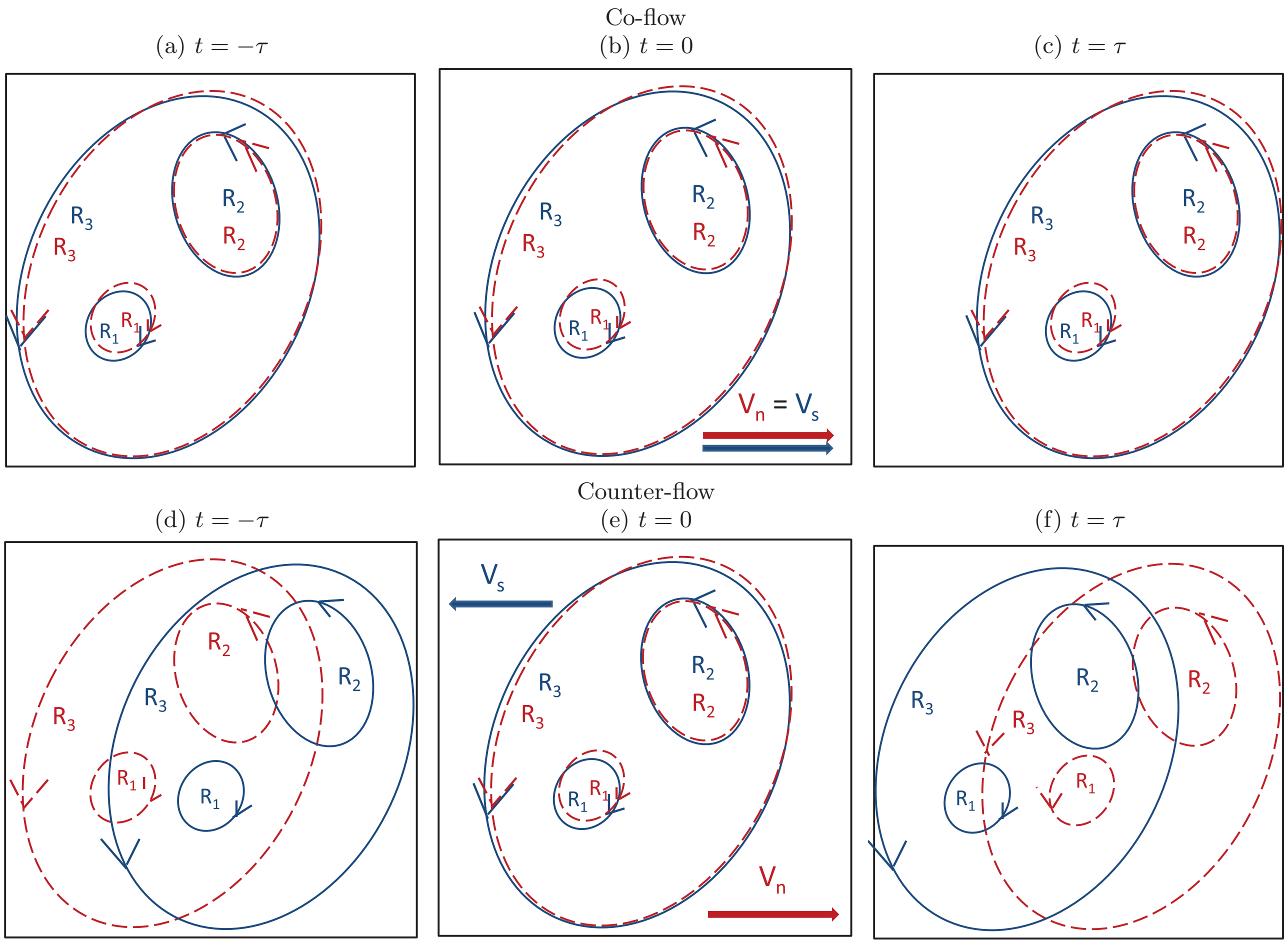

FIG. 1. Schematic view of the normal-fluid eddies of scales R_1, R_2, and R_3 (red dashed lines), swept by the mean normal-fluid velocity U_n, and of the superfluid eddies of the same scales (blue solid lines) swept by the mean superfluid velocity U_s in (a)–(c) the coflow with $\boldsymbol{U}_n = \boldsymbol{U}_s$ and (d)–(f) the counterflow with $U_{ns} = |\boldsymbol{U}_n - \boldsymbol{U}_s| \neq 0$, at three consequent moments of time: (a),(d) $t = -\tau$, (b),(e) $t = 0$, and (c),(f) $t = \tau$. The time interval $\tau \simeq R_2/U_{ns}$ is of the order of overlapping time of the middle-scale R_2 eddies.

(red dashed line) eddies are moving in our pictures from the left [in Fig. 1(d)] to the right [in Fig. 1(f)]. At the same time, $U_s < 0$ and superfluid (blue solid line) eddies are moving in the opposite direction.

Assume that at some intermediate moment of time [chosen as $t = 0$ in Fig. 1(e)], all normal- and superfluid eddies of scales R_1, R_2, and R_3 overlap. Choose the time step τ, such that $\tau \simeq R_2/U_{ns}$. The largest eddies of scale R_3 are almost fully overlapping during the time step τ, while smaller eddies of scale R_1, which were overlapping at $t = 0$, are fully separated at times $t \pm \tau$. Intermediate R_2-scale eddies are partially overlapping during the time step $\tau \simeq \tau_{ol}(R_2)$. Here the "overlapping time" of R eddies $\tau_{ol}(R) = R/U_{ns}$ is the time that is required for eddies to be swept by the counterflow velocity U_{ns} over the distance of their scale R.

This time may be small compared to the time τ_{cor} required for an effective coupling of the $\boldsymbol{u}_s(\boldsymbol{r},t)$ and $\boldsymbol{u}_n(\boldsymbol{r},t)$ velocities. As we show in the last paragraph of Sec. II B, τ_{cor} is scale independent and may be estimated as $\tau_{cor} \sim 1/(\kappa\mathcal{L})$, where $\mathcal{L}$ is the vortex line density. The detailed analysis shows that for most eddies in the relevant range of scales $H < R < \ell$, the time $\tau_{ol} \ll \tau_{cor}$ and therefore the velocities $\boldsymbol{u}_s(\boldsymbol{r},t)$ and $\boldsymbol{u}_n(\boldsymbol{r},t)$ are decoupled. This makes the energy dissipation due to mutual friction very effective and results in significant suppression of the energy spectra of the normal- and superfluid turbulent velocity spectra as compared to that in the mechanically driven turbulence, in which $U_{ns} = 0$.

Notice that in Ref. [15], it was mentioned that in the counterflow, the coupling at all length scales must, to some extent, break down because similar eddies in the two components are continually pulled apart, and this leads to dissipation at all length scales.

The main goal of the present paper is to offer a relatively simple, physically transparent model of the cross-correlation function of the normal- and superfluid velocities, which accounts for the nonzero value of the mean counterflow velocity U_{ns}. For simplicity, we consider only the case of homogeneous and isotropic turbulence of an incompressible flow of ^{4}He. In this flow, the difference between the counterflow and a pure superflow turbulence disappears due to Galilean invariance. The paper is organized as follows. First, we overview the two-fluid coarse-grained Hall-Vinen-Bekarevich-Khalatnikov (HVBK) model [8,16], properly generalized for the case of counterflow turbulence, given by Eqs. (3). Second, we suggest an approach that leads to a crucial simplification that allows us to derive analytical equations (14) for the cross-correlation function of the normal- and superfluid velocity fluctuations, $\mathcal{E}_{ns}(k,U_{ns})$. Third, we analyze the equation for $\mathcal{E}_{ns}(k,U_{ns})$ and show that as a rule, $\mathcal{E}_{ns}(k,U_{ns}) \ll \mathcal{E}_{ns}(k,0)$; see Fig. 3. Finally, in the concluding section, we discuss how the decoupling of velocities should affect the normal- and superfluid energy spectra.

II. BASIC EQUATIONS OF MOTION FOR COUNTERFLOW TURBULENCE

A. Two-fluid, gradually damped HVBK equations

As said above, the large-scale motions of superfluid ^{4}He (with characteristic scales $R \gg \ell$) are well described by the two-fluid model, consisting of a normal-fluid and a superfluid component with densities $\rho_n(T)$ and $\rho_s(T)$, respectively. Neglecting both the bulk viscosity and the thermal conductivity leads to the simplest model with two incompressible fluids, with the form of an Euler equation for $\boldsymbol{u}_s$ and a Navier-Stokes equation for $\boldsymbol{u}_n$; see, e.g., Eqs. (2.2) and (2.3) in Ref. [1]. Supplemented with quantized vortices that give rise to a mutual friction force $\boldsymbol{F}_{ns}$ between the superfluid and the normal-fluid components, these equations are known as the HVBK model [8,16]:

$$\frac{\partial \boldsymbol{u}_s}{\partial t} + (\boldsymbol{u}_s \cdot \nabla)\boldsymbol{u}_s + \frac{1}{\rho_s}\nabla p_s = \nu_s' \,\Delta \boldsymbol{u}_s - \boldsymbol{F}_{ns}, \tag{2a}$$

$$\frac{\partial \boldsymbol{u}_n}{\partial t} + (\boldsymbol{u}_n \cdot \nabla)\boldsymbol{u}_n + \frac{1}{\rho_n}\nabla p_n = \nu_n \,\Delta \boldsymbol{u}_n + \frac{\rho_s}{\rho_n}\boldsymbol{F}_{ns}. \tag{2b}$$

Here, p_n, p_s are the pressures of the normal-fluid and the superfluid components,

$$p_n = \frac{\rho_n}{\rho}\Big[p + \frac{\rho_s}{2}|\boldsymbol{u}_s - \boldsymbol{u}_n|^2\Big], \quad p_s = \frac{\rho_s}{\rho}\Big[p - \frac{\rho_n}{2}|\boldsymbol{u}_s - \boldsymbol{u}_n|^2\Big],$$

$\rho \equiv \rho_s + \rho_n$ is the total density, and ν_n is the kinematic viscosity of normal fluid. The mutual friction force is given by

$$\boldsymbol{F}_{ns} = \alpha\, \hat{\boldsymbol{\omega}} \times [\boldsymbol{\omega} \times (\boldsymbol{u}_n - \boldsymbol{u}_s)] + \alpha' \hat{\boldsymbol{\omega}} \times (\boldsymbol{u}_n - \boldsymbol{u}_s).$$

In this equation, α,α' are temperature-dependent dimensionless mutual friction parameters and $\boldsymbol{\omega}$ is traditionally understood as the superfluid vorticity: $\boldsymbol{\omega} = \nabla \times \boldsymbol{u}_s$ and $\hat{\omega} \equiv \boldsymbol{\omega}/|\boldsymbol{\omega}|$.

Notice also that the original HVBK model does not take into account the important process of vortex reconnection. In fact, vortex reconnections are responsible for the dissipation of the superfluid motion due to mutual friction.

For temperatures above 1 K, this extra dissipation can be modeled using an effective superfluid viscosity $\nu_s'(T)$ [17],

$$\nu_s'(T) \approx \alpha\kappa, \tag{2c}$$

and, following Ref. [13], we have added a dissipative term proportional to ν_s' to the standard HVBK model.

The effective superfluid viscosity ν_s' involves a quantum-mechanical parameter κ, proportional to the Plank's constant h. This underlies the fact that the corresponding term in Eqs. (2) originates from the motions of quantized vortex lines at quantum scales $\sim \ell$. This is not captured by the coarse-grained, classical HVBK equations.

Bearing in mind that experimentally the counterflow cannot be realized for $T < 1$ K (due to practically zero normal-fluid density), we cannot discuss here the delicate issue of how to account for the superfluid dissipation in Eqs. (2) for such low temperatures.

B. Counterflow HVBK equations

To proceed, we separate the mean velocities $\boldsymbol{U}_n$ and $\boldsymbol{U}_s$ from the turbulent velocity fluctuations, $\boldsymbol{u}_n'(\boldsymbol{r},t)$ and $\boldsymbol{u}_s'(\boldsymbol{r},t)$, with zero mean. Equations (2) for $\boldsymbol{u}_n'(\boldsymbol{r},t)$ and $\boldsymbol{u}_s'(\boldsymbol{r},t)$ may be written as follows:

$$\left(\frac{\partial}{\partial t} + \boldsymbol{U}_s \cdot \nabla - \nu_s' \,\Delta\right)\boldsymbol{u}_s' + \mathrm{NL}\{\boldsymbol{u}_s',\boldsymbol{u}_s'\} = -\boldsymbol{f}_{ns}', \tag{3a}$$

$$\left(\frac{\partial}{\partial t} + \boldsymbol{U}_n \cdot \nabla - \nu_n \,\Delta\right)\boldsymbol{u}_n' + \mathrm{NL}\{\boldsymbol{u}_n',\boldsymbol{u}_n'\} = \frac{\rho_s}{\rho_n}\boldsymbol{f}_{ns}'. \tag{3b}$$

Here the nonlinear terms $\mathrm{NL}\{\boldsymbol{u}_s',\boldsymbol{u}_s'\}$ and $\mathrm{NL}\{\boldsymbol{u}_n',\boldsymbol{u}_n'\}$ are quadratic in the corresponding velocities functionals. These terms originate from the terms $\boldsymbol{u}' \cdot \nabla \boldsymbol{u}'$ and from the $\nabla p'$ terms, where the pressure fluctuations $p'(\boldsymbol{r},t)$ were expressed via a quadratic velocity fluctuation functional, using the incompressibility condition. For our purpose, we will not need to specify the nonlinear terms $\mathrm{NL}\{\boldsymbol{u}_s',\boldsymbol{u}_s'\}$ and $\mathrm{NL}\{\boldsymbol{u}_n',\boldsymbol{u}_n'\}$.

Next we approximate the mutual friction fluctuation term $\boldsymbol{f}_{ns}'$. In the spirit of Ref. [18], we write as follows:

$$\boldsymbol{f}_{ns}' \simeq -\alpha(T)\,(\boldsymbol{u}_n' - \boldsymbol{u}_s')\Omega. \tag{3c}$$

In Ref. [18], the characteristic superfluid vorticity Ω in Eq. (3c) was understood as the root-mean-square (rms) vorticity: $\Omega \simeq \sqrt{\langle|\boldsymbol{\omega}|^2\rangle}$. However, in counterflow turbulence, there is an additional quantum mechanism of creating vortex lines, elucidated in pioneering works by Schwarz [19]: the force of mutual friction can lead to the stretching of the vortex lines, and this in turn can lead to a self-sustaining turbulence in the superfluid component provided that vortex lines are allowed to reconnect. This mechanism is leading to the creation of an additional peak in the superfluid energy spectrum near the intervortex scale ℓ, sketched in Fig. 2. In the counterflowing superfluid turbulence, this peak provides the main contribution to the rms vorticity, which cannot be described in the framework of the coarse-grained HVBK of Eqs. (3a) and (3b), which is valid only for scales $R \gg \ell$. Therefore, Ω in Eq. (3c) should be understood as an external parameter in the HVBK equations for the counterflow, simply estimated via the vortex line density $\mathcal{L}$, which in its turn is proportional to the square of the counterflow velocity:

$$\Omega \simeq \kappa\mathcal{L}, \quad \mathcal{L} \approx (\gamma_{\mathcal{L}} U_{ns})^2. \tag{3d}$$

Here, $\gamma_{\mathcal{L}}$ is a temperature-dependent phenomenological parameter that varies from about 70 s/cm^2 to about 150 s/cm^2 when T grows from 1.3 to 1.9 K (see, e.g., Fig. 9 in Ref. [20]). Here we have added a subscript $_{\mathcal{L}}$ to distinguish the traditional notation γ in Eq. (3d) from the characteristic frequencies γ_s and γ_n that are used below.

The resulting gradually damped HVBK model for turbulent counterflow in ^{4}He, given by Eqs. (3), serves as a basis for our study of the correlations between normal- and superfluid velocity correlations. We will refer to these equations as the "counterflow HVBK equations."

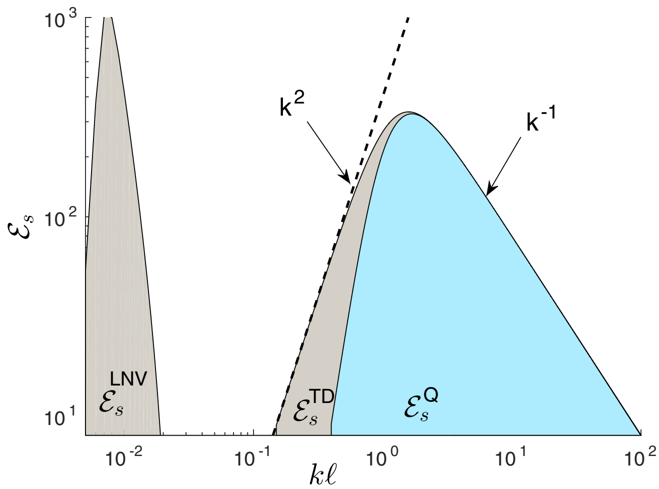

FIG. 2. The sketch of the stationary superfluid turbulent energy spectrum in the counterflow [log-log coordinates, $\log \mathcal{E}_s(k)$ vs $\log(k\ell)$]. The spectrum $\mathcal{E}_s(k)$ consists of a classical $\mathcal{E}_s^{cl}(k)$ and a quantum $\mathcal{E}_s^{qn}(k)$ part, colored in gray and light blue, respectively. For concreteness, as a large-scale classical peak, we used the Lvov-Nazarenko-Volovik spectrum (19), found for ^{3}He with resting normal-fluid component, but presumably valid for counterflowing ^{4}He in the k range with fully decoupled normal- and superfluid velocities. The quantum (light blue) contribution $\mathcal{E}_s^{Q}(k)$ has $1/k$ asymptotics at large k, originated from superfluid motions near the vortex cores. It is adjacent to the classical thermal bath part $\mathcal{E}_s^{TD}(k) \propto k^2$, with equipartition of energy between degrees of freedoms.

Equations (3) allow one to estimate the time τ_{cor} required for the coupling of the normal- and superfluid turbulent velocities by mutual friction. To this end, we consider an equation for their difference, $\boldsymbol{u}'_{ns} \equiv \boldsymbol{u}'_n - \boldsymbol{u}'_s$, subtracting Eq. (3a) from Eq. (3b):

$$\frac{\partial\, \boldsymbol{u}'_{ns}}{\partial t} + \cdots = -(\kappa\mathcal{L})\,\alpha_{ns}\boldsymbol{u}'_{ns}, \quad \alpha_{ns} \equiv \frac{\alpha\rho}{\rho_n}.$$

Here we denoted by $\cdots$ the sweeping, viscous, and nonlinear terms that are irrelevant for the current discussion. Evidently, τ_{cor} should be estimated as $1/(\alpha_{ns}\kappa\mathcal{L})$. The temperature dependence of α_{ns}, shown in Fig. 4 by a red line with squares, indicates that $\alpha_{ns} \sim 1$. Therefore, we can conclude that $\tau_{cor} \sim 1/(\kappa\mathcal{L})$, as mentioned in Sec. I.

III. NORMAL- AND SUPERFLUID VELOCITY CORRELATIONS IN ^{4}He

The main result of this section is Eq. (14) for the cross-correlation function of the normal- and superfluid velocity turbulent fluctuations in a stationary, space homogenous counterflow ^{4}He turbulence. This equation describes how the cross correlations depend on the counterflow velocity, the scale (wave number), and the temperature. Its derivation requires some definitions and relationships that are common in statistical physics. We recall them in Appendix.

A. Derivation of the cross correlation $\mathcal{E}_{ns}(k)$

The first step in the derivation of the cross correlation is rewriting the counterflow HVBK given by Eqs. (3) in $(\boldsymbol{k},t)$ representation, defined by Eq. (A1a):

$$\left(\frac{\partial}{\partial t} + i\boldsymbol{U}_s\cdot\boldsymbol{k} + \nu'_s k^2 + \Omega_s\right)\boldsymbol{v}_s + \mathrm{NL}_{\boldsymbol{k}}\{\boldsymbol{v}_s,\boldsymbol{v}_s\} = \Omega_s\boldsymbol{v}_n, \tag{4a}$$

$$\left(\frac{\partial}{\partial t} + i\boldsymbol{U}_n\cdot\boldsymbol{k} + \nu_n k^2 + \Omega_n\right)\boldsymbol{v}_n + \mathrm{NL}_{\boldsymbol{k}}\{\boldsymbol{v}_n,\boldsymbol{v}_n\} = \Omega_n\boldsymbol{v}_s, \tag{4b}$$

where the mutual friction frequencies are given by

$$\Omega_s \equiv \alpha\Omega, \quad \Omega_n \equiv \alpha_n\Omega, \quad \alpha_n \equiv \alpha\,\rho_s/\rho_n. \tag{4c}$$

The nonlinear terms $\mathrm{NL}_{\boldsymbol{k}}\{\boldsymbol{v}_s,\boldsymbol{v}_s\}$ and $\mathrm{NL}_{\boldsymbol{k}}\{\boldsymbol{v}_n,\boldsymbol{v}_n\}$ in Eqs. (4a) and (4b) couple all $\boldsymbol{k}$-Fourier harmonics, making their analytic solution intractable. To proceed, we therefore simplify the equations in the spirit of the direct interaction approximation (DIA) that was developed by Kraichnan for classical turbulence [21]. This approximation is equivalent to a one-loop truncation of the Wyld diagrammatic expansion [22] of the nonlinear equations with a one-pole approximation [23] for the Green's function. While uncontrolled, this approximation has served usefully in the study of classical turbulence, and we propose that it is also useful in the present context. The upshot of the DIA is a rewriting of the nonlinear terms in Eqs. (4a) and (4b) as a sum of two contributions [24]:

$$\mathrm{NL}_{\boldsymbol{k}}\{\boldsymbol{v}_s,\boldsymbol{v}_s\} = \gamma_s(k)\boldsymbol{v}_s(\boldsymbol{k},t) - \boldsymbol{\varphi}_s(\boldsymbol{k},t), \tag{5a}$$

$$\mathrm{NL}_{\boldsymbol{k}}\{\boldsymbol{v}_n,\boldsymbol{v}_n\} = \gamma_n(k)\boldsymbol{v}_n(\boldsymbol{k},t) - \boldsymbol{\varphi}_n(\boldsymbol{k},t). \tag{5b}$$

The $\gamma_s(k)$ and $\gamma_n(k)$ are the characteristic frequencies and $\boldsymbol{\varphi}_s(\boldsymbol{k},t)$ and $\boldsymbol{\varphi}_n(\boldsymbol{k},t)$ are the force terms. The terms proportional to $\gamma_s(k)$ and $\gamma_n(k)$ describe the energy flux from fluctuations with given $\boldsymbol{k}$ to all others degrees of freedom. In classical turbulence theory, these characteristic frequencies are referred to as "turbulent viscosity" and estimated as follows:

$$\gamma_n(k) \simeq \sqrt{k^3\mathcal{E}_n(k)}, \quad \gamma_s(k) \simeq \sqrt{k^3\mathcal{E}_s(k)}. \tag{5c}$$

In turbulent systems with strong interactions, these frequencies are the inverse turnover times of eddies of scale $1/k$.

The force terms in the approximation (5a) and (5b) mimic the energy influx to fluctuations with given $\boldsymbol{k}$ from all others degrees of freedom. In the simplest Langevin approach, these forces are random Gaussian processes with zero mean and are δ correlated in time:

$$\begin{aligned}
\langle\boldsymbol{\varphi}_s(\boldsymbol{k},t)\cdot\boldsymbol{\varphi}_s^*(\boldsymbol{k}',t')\rangle &= (2\pi)^3\delta(\boldsymbol{k}-\boldsymbol{k}')\delta(t-t')\varphi_{ss}^2(\boldsymbol{k}),\\
\langle\boldsymbol{\varphi}_n(\boldsymbol{k},t)\cdot\boldsymbol{\varphi}_n^*(\boldsymbol{k}',t')\rangle &= (2\pi)^3\delta(\boldsymbol{k}-\boldsymbol{k}')\delta(t-t')\varphi_{nn}^2(\boldsymbol{k}),\\
\langle\boldsymbol{\varphi}_s(\boldsymbol{k},t)\cdot\boldsymbol{\varphi}_n^*(\boldsymbol{k}',t')\rangle &= 0.
\end{aligned} \tag{5d}$$

Here the δ functions, $\delta(\boldsymbol{k}-\boldsymbol{k}')$, originate from the space homogeneity. An important difference from the traditional Langevin approach is that our turbulent system is not in the thermodynamic equilibrium and therefore the correlation amplitudes φ_{nn}^2 and φ_{ss}^2 are not determined by fluctuation-dissipation theorems. We will show below that these amplitudes may be expressed via the energy spectra $\mathcal{E}_s(k)$ and $\mathcal{E}_n(k)$.

With these approximations, the counterflow HVBK given by Eqs. (4) become linear in $\boldsymbol{v}_s$ and $\boldsymbol{v}_n$:

$$\left[\frac{\partial}{\partial t} + i\boldsymbol{k}\cdot\boldsymbol{U}_s + \Gamma_s\right]\boldsymbol{v}_s(\boldsymbol{k},t) = \Omega_s \boldsymbol{v}_n(\boldsymbol{k},t) + \boldsymbol{\varphi}_s(\boldsymbol{k},t), \quad (6a)$$

$$\left[\frac{\partial}{\partial t} + i\boldsymbol{k}\cdot\boldsymbol{U}_n + \Gamma_n\right]\boldsymbol{v}_n(\boldsymbol{k},t) = \Omega_n \boldsymbol{v}_s(\boldsymbol{k},t) + \boldsymbol{\varphi}_n(\boldsymbol{k},t), \quad (6b)$$

$$\Gamma_n = \gamma_n + \Omega_n + \nu_n k^2, \quad \Gamma_s = \gamma_s + \Omega_s + \nu_s' k^2. \quad (6c)$$

Clearly, counterflow turbulence in a channel is anisotropic due to the existence of two preferred directions: the streamwise direction $\boldsymbol{x}$ and the wall-normal direction $\boldsymbol{y}$. Even far away from the wall, in the channel core, where classical hydrodynamic turbulence can be treated as isotropic, in quantum turbulence there remains one preferred direction $\boldsymbol{x}$ of the counterflow velocity $\boldsymbol{U}_{ns}$. Schwarz [19] introduced an anisotropy index $I_\parallel$, equal to $2/3$ in the case of isotropy. Numerical simulations (see, e.g., Ref. [25]) show that $I_\parallel$ varies between 0.74 and 0.82, depending on the temperature and the counterflow velocity. Therefore, the dimensionless measure of anisotropy $3I_\parallel/2 - 1$ is below 20% in any case. According to our understanding, this level of anisotropy cannot significantly affect the results presented below. Aiming at simplicity and transparency of the derivation, we assume isotropy from the very beginning, leaving a more general derivation (in the framework of the same formal scheme) for the future. For weak anisotropy, all of our results should be understood as angular averages.

Multiplying Eqs. (6a) and (6b) by $\boldsymbol{v}_s^*$, and $\boldsymbol{v}_n^*$, respectively, and averaging, we get equations for the velocity correlations E_{nn}, E_{ss} and the cross correlation E_{ns}, defined by Eqs. (A4):

$$\left[\frac{\partial}{2\,\partial t} + \Gamma_s\right]E_{ss} = \Omega_s \mathrm{Re}[E_{ns}] + \mathrm{Re}[\Phi_{ss}], \quad (7a)$$

$$\left[\frac{\partial}{2\,\partial t} + \Gamma_n\right]E_{nn} = \Omega_n \mathrm{Re}[E_{ns}] + \mathrm{Re}[\Phi_{nn}], \quad (7b)$$

$$\left[\frac{\partial}{\partial t} + i\boldsymbol{k}\cdot\boldsymbol{U}_{ns} + \Gamma_s + \Gamma_n\right]E_{ns} = [\Omega_s E_{nn} + \Omega_n E_{ss}] + \Phi_{sn}^* + \Phi_{ns}. \quad (7c)$$

These equations involve the presently unknown simultaneous cross correlations of the velocities and the forces, $\Phi_{\dots}$, defined similarly to Eqs. (A2):

$$\langle \boldsymbol{\varphi}_n(\boldsymbol{k},t)\cdot \boldsymbol{v}_n^*(\boldsymbol{k}',t)\rangle = (2\pi)^3 \Phi_{nn}(\boldsymbol{k})\,\delta(\boldsymbol{k}-\boldsymbol{k}'), \quad (8a)$$

$$\langle \boldsymbol{\varphi}_s(\boldsymbol{k},t)\cdot \boldsymbol{v}_s^*(\boldsymbol{k}',t)\rangle = (2\pi)^3 \Phi_{ss}(\boldsymbol{k})\,\delta(\boldsymbol{k}-\boldsymbol{k}'), \quad (8b)$$

$$\langle \boldsymbol{\varphi}_n(\boldsymbol{k},t)\cdot \boldsymbol{v}_s^*(\boldsymbol{k}',t)\rangle = (2\pi)^3 \Phi_{ns}(\boldsymbol{k})\,\delta(\boldsymbol{k}-\boldsymbol{k}'), \quad (8c)$$

$$\langle \boldsymbol{\varphi}_s(\boldsymbol{k},t)\cdot \boldsymbol{v}_n^*(\boldsymbol{k}',t)\rangle = (2\pi)^3 \Phi_{sn}(\boldsymbol{k})\,\delta(\boldsymbol{k}-\boldsymbol{k}'). \quad (8d)$$

To find these correlations, we rewrite Eqs. (6) in Fourier $(\boldsymbol{k},\omega)$ representation,

$$[i(\boldsymbol{k}\cdot\boldsymbol{U}_s - \omega) + \Gamma_s]\widetilde{\boldsymbol{v}}_s(\boldsymbol{k},\omega) = \Omega_s \widetilde{\boldsymbol{v}}_n(\boldsymbol{k},\omega) + \widetilde{\boldsymbol{\varphi}}_s(\boldsymbol{k},\omega), \quad (9a)$$

$$[i(\boldsymbol{k}\cdot\boldsymbol{U}_n - \omega) + \Gamma_n]\widetilde{\boldsymbol{v}}_n(\boldsymbol{k},\omega) = \Omega_n \widetilde{\boldsymbol{v}}_s(\boldsymbol{k},\omega) + \widetilde{\boldsymbol{\varphi}}_n(\boldsymbol{k},\omega), \quad (9b)$$

where $\widetilde{\boldsymbol{\varphi}}_s(\boldsymbol{k},\omega)$ and $\widetilde{\boldsymbol{\varphi}}_n(\boldsymbol{k},\omega)$ are the $(\boldsymbol{k},\omega)$ representation of the force terms $\boldsymbol{\varphi}_s(\boldsymbol{k},t)$ or $\boldsymbol{\varphi}_n(\boldsymbol{k},t)$. The solution of the linear Eqs. (9) reads

$$\widetilde{\boldsymbol{v}}_s = -\{[i(\boldsymbol{k}\cdot\boldsymbol{U}_n - \omega) + \Gamma_n]\widetilde{\boldsymbol{\varphi}}_s + \Omega_s\widetilde{\boldsymbol{\varphi}}_n\}/\Delta, \quad (10a)$$

$$\widetilde{\boldsymbol{v}}_n = -\{[i(\boldsymbol{k}\cdot\boldsymbol{U}_s - \omega) + \Gamma_s]\widetilde{\boldsymbol{\varphi}}_n + \Omega_n\widetilde{\boldsymbol{\varphi}}_s\}/\Delta, \quad (10b)$$

$$\Delta \equiv (\omega - \boldsymbol{k}\cdot\boldsymbol{U}_n + i\Gamma_n)(\omega - \boldsymbol{k}\cdot\boldsymbol{U}_s + i\Gamma_s) + \Omega_n\Omega_s, \quad (10c)$$

where for brevity we suppressed the arguments $(\boldsymbol{k},\omega)$ in all functions.

Multiplying the two Eqs. (10) by $\widetilde{\boldsymbol{\varphi}}_n$ and $\widetilde{\boldsymbol{\varphi}}_s$, respectively, and averaging, we get equations for the (cross) correlations $\widetilde{\Phi}_{ns}(\boldsymbol{k},\omega)$ and $\widetilde{\Phi}_{sn}(\boldsymbol{k},\omega)$, which give after integration over ω the simultaneous cross-correlation functions,

$$\Phi_{sn}(\boldsymbol{k}) = -\frac{\Omega_s f_n^2}{2\pi}\int \frac{d\omega}{\Delta^*(\boldsymbol{k},\omega)} = 0, \quad (11a)$$

$$\Phi_{ns}(\boldsymbol{k}) = -\frac{\Omega_n f_s^2}{2\pi}\int \frac{d\omega}{\Delta^*(\boldsymbol{k},\omega)} = 0. \quad (11b)$$

To compute the above integrals, we found the solutions of the equations $\Delta(\boldsymbol{k},\omega) = 0$ with respect to ω,

$$\omega = \omega_\pm = \frac{i}{2}[-i\boldsymbol{k}\cdot(\boldsymbol{U}_n + \boldsymbol{U}_s) + \Gamma_s + \Gamma_n] \pm \sqrt{(\Gamma_s - \Gamma_n + i\boldsymbol{k}\cdot\boldsymbol{U}_{ns})^2 + 4\Omega_s\Omega_n}. \quad (12)$$

Using these solutions, after relatively simple analysis, we find that both roots have positive imaginary parts: $\mathrm{Im}[\omega_+] > 0$ and $\mathrm{Im}[\omega_-] > 0$. Therefore, the integral in Eqs. (11) vanishes. Now Eq. (7c) in the stationary case gives

$$E_{ns}(\boldsymbol{k}) = \frac{A}{B + i\boldsymbol{k}\cdot\boldsymbol{U}_{ns}}, \quad (13a)$$

$$A \equiv \Omega_s E_{nn}(k) + \Omega_n E_{ss}(k), \quad (13b)$$

$$B \equiv \Gamma_n + \Gamma_s. \quad (13c)$$

Averaging Eq. (13a) with respect to all orientations of $\boldsymbol{k}$, we get

$$\langle E_{ns}(\boldsymbol{k})\rangle_{\text{angle}} = \frac{A}{kU_{ns}}\arctan\left(\frac{kU_{ns}}{B}\right). \quad (13d)$$

Using Eqs. (A5), this can finally be rewritten as follows:

$$\mathcal{E}_{ns}(k) = \mathcal{E}_{ns}^{(0)}(k)D(\zeta), \quad (14a)$$

$$\mathcal{E}_{ns}^{(0)}(k) = \frac{\Omega_s\mathcal{E}_n(k) + \Omega_n\mathcal{E}_s(k)}{\Gamma_s(k) + \Gamma_n(k)}, \quad (14b)$$

$$D(\zeta) = \frac{1}{\zeta(k)}\arctan[\zeta(k)], \quad (14c)$$

$$\zeta(k) \equiv \frac{kU_{ns}}{\Gamma_s(k) + \Gamma_n(k)}. \quad (14d)$$

Here, $\mathcal{E}_{ns}^{(0)}(k)$ is the cross-correlation function for zero counterflow velocity, which was previously found in Ref. [10]. The dimensionless "decoupling function" $D(\zeta)$ of the dimensionless "decoupling parameter" $\zeta(k)$ describes the decoupling of the normal- and superfluid velocity fluctuations, caused by the counterflow velocity.

Notice that in future comparisons of the experimental or numerical data with Eqs. (14), one needs to bear in mind

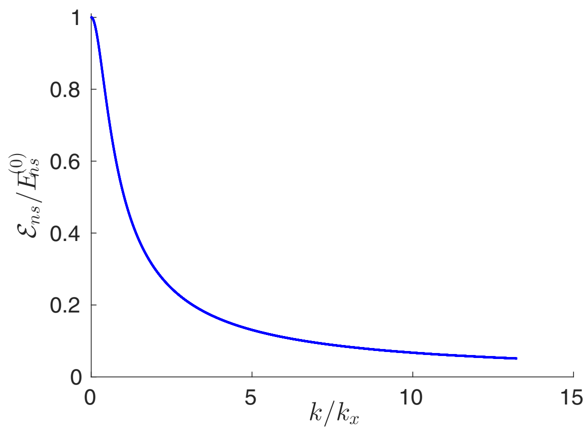

FIG. 3. The decoupling function $\mathcal{E}_{\rm ns}/\mathcal{E}^{(0)}_{\rm ns} = D(k/k_\times)$ vs the dimensionless wave number $k/k_\times$.

that the counterflow velocity affects not only the decoupling function $D(\xi)$, but also the energy spectra $\mathcal{E}_{\rm n}(k)$ and $\mathcal{E}_{\rm s}(k)$ in Eq. (14b) for $\mathcal{E}^{(0)}_{\rm ns}(k)$.

Considering the limits of small and large values of the decoupling parameter ζ, we get, from Eq. (14a),

$$\mathcal{E}_{\rm ns}(k) = \left[1 - \frac{\zeta(k)^2}{3}\right]\mathcal{E}^{(0)}_{\rm ns}(k) \quad \text{for } \zeta(k) \ll 1, \tag{15a}$$

$$\mathcal{E}_{\rm ns}(k) = \frac{\pi}{2\,\zeta(k)}\,\mathcal{E}^{(0)}_{\rm ns}(k) \quad \text{for } \zeta(k) \gg 1. \tag{15b}$$

We choose the crossover value $\zeta_\times \approx 2$ such that $D(\zeta_\times) = 1/2$. Below we show that with good accuracy, $\zeta(k) \propto k$. Therefore, we can consider $D[\zeta(k)]$ as a function of k and present in Fig. 3 the decoupling ratio due to counterflow velocity $\mathcal{E}_{\rm ns}(k)/\mathcal{E}^{(0)}_{\rm ns}(k) = D[\zeta(k)]$, as a function of $k/k_\times$. Our estimate below shows that the crossover wave number $k_\times$ [for which $\mathcal{E}_{\rm ns}(k) = \mathcal{E}^{(0)}_{\rm ns}(k)/2$] is independent of the counterflow velocity and typically is in the relevant interval of scales, between π/H and π/ℓ.

B. Typical value of the decoupling parameter $\zeta(k)$

To clarify what the typical values of $\zeta(k)$ are in realistic conditions and how $\zeta(k)$ depends on the temperature and the counterflow velocity, we note [20] that the main contributions to $\Gamma_{\rm n}$ and $\Gamma_{\rm s}$, given by Eq. (6c), come from $\Omega_{\rm n}$ and $\Omega_{\rm s}$, given by Eq 6(c):

$$\Gamma_{\rm n} + \Gamma_{\rm s} \approx \Omega_{\rm n} + \Omega_{\rm s} = \alpha_{\rm ns}\,\Omega, \quad \alpha_{\rm ns} = \alpha + \alpha_{\rm n} = \frac{\alpha\,\rho}{\rho_{\rm n}}. \tag{16}$$

Indeed, for scales $k\ell \ll 1$, the viscous terms $\nu_{\rm s,n}k^2 \gg \gamma_{\rm s,n}(k)$ and may be safely neglected, while for scales near the intervortex distance, they are of the same order of magnitude. Moreover, for $k\ell \sim 1, \nu_{\rm s,n}k^2 \sim \gamma_{\rm s,n}(k) \sim \Omega_{\rm s,n}$, if one estimates $\Omega_{\rm s,n} \sim \Omega_{\rm cl}$ in a classical manner via the root mean square of the vorticity (see, e.g., Refs. [13,18]), then $\Omega_{\rm cl} \sim \sqrt{\langle\omega^2\rangle}$. However, as we explained above, in the counterflow there is an additional quantum mechanism of the random vortex tangle excitation with scales of the order of ℓ. This mechanism provides the leading contribution to $\Omega_{\rm s,n}$ and, consequently, the leading contribution to $\Gamma_{\rm s,n}$, as written in Eq. (16).

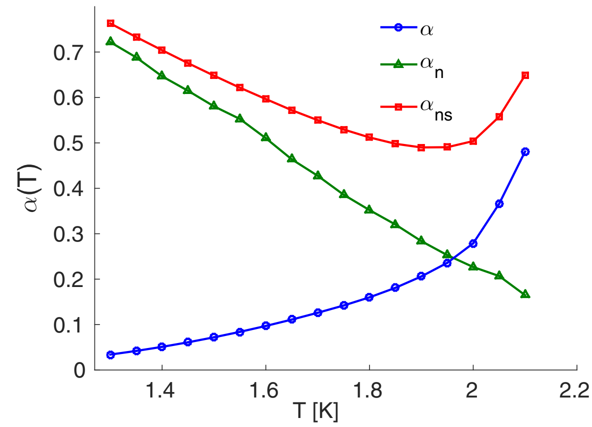

FIG. 4. Temperature dependence of the mutual friction parameters for ^{4}He (Ref. [26]): α for the superfluid given by Eq. (3a) (blue line with circles); $\alpha_{\rm n}(T) = \alpha\rho_{\rm s}/\rho_{\rm n}$ in the normal fluid given by Eq. (3b) (green line with triangles); and $\alpha_{\rm ns} = \alpha + \alpha_{\rm n} = \alpha\rho/\rho_{\rm n}$ given by Eqs. (16) (red line with squares).

The temperature dependence of $\alpha_{\rm ns}(T) = B(T)/2$, where $B(T)$ is the coefficient in the Vinen equation, tabulated in Ref. [26], is shown in Fig. 4 together with $\alpha(T)$ and $\alpha_{\rm n}(T)$. The opposite temperature dependence of $\alpha(T)$ and $\alpha_{\rm n}(T)$ results in a weak temperature dependence of the parameter $\alpha_{\rm ns}(T)$ in Eq. (16); it varies between 0.7 and 0.5 in the temperature range that is relevant for counterflow experiments, $1.4 \div 1.9$ K.

Now Eqs. (3d) and (16) together with Eq. (14d) give

$$\zeta(k) \simeq \frac{k}{\alpha_{\rm ns}\kappa\gamma^2_{\mathcal{L}}U_{\rm ns}}. \tag{17a}$$

Clearly, $\zeta(k) \propto k$ and it reaches its maximal value $\zeta_{\rm max}$ at the highest k value which is permissible in our approach, i.e., $k \simeq k_{\rm max} \simeq \pi/\ell$; this is at the edge of the applicability. With $\ell \simeq 1/\sqrt{\mathcal{L}} \simeq 1/(\gamma_{\mathcal{L}}U_{\rm ns})$, this gives a simple estimate of $\zeta_{\rm max}$, independent of $U_{\rm ns}$:

$$\zeta_{\rm max} \simeq \frac{\pi}{\alpha_{\rm ns}\,\kappa\,\gamma_{\mathcal{L}}} \sim 50 \quad \text{for } T \approx 1.4 \text{ K}. \tag{17b}$$

Here, for the numerical estimate, we used $\alpha_{\rm ns} \simeq 0.6$, $\gamma_{\mathcal{L}} \simeq 100$ s/cm^2, and $\kappa \approx 10^{-3}$ cm^2/s. An important conclusion is that for large k, the normal- and superfluid velocities are practically fully decoupled: for $k \sim k_{\rm max}$ $\zeta(k) \sim 50$ and the ratio $\mathcal{E}_{\rm ns}/\mathcal{E}^{(0)}_{\rm ns}$ is about 0.03 according to Eq. (15b).

An even more important conclusion is that according to Eq. (17b), the range of wave numbers $k_{\rm max} > k > k_\times$, where $\mathcal{E}_{\rm ns}/\mathcal{E}^{(0)}_{\rm ns} < 1/2$, extends over more than one decade:

$$\frac{\zeta_{\rm max}}{\zeta_\times} \simeq \frac{k_{\rm max}}{k_\times} \simeq \frac{\pi}{2\alpha_{\rm ns}\,\kappa\,\gamma_{\mathcal{L}}} \sim 25 \quad \text{for } T \approx 1.4 \text{ K}. \tag{17c}$$

Equation (17a) allows us to also estimate the minimal value $\zeta_{\rm min}$, which is attained at $k_{\rm min} \simeq \pi/H$:

$$\zeta_{\rm min} \simeq \frac{\pi}{H\alpha_{\rm ns}\kappa\gamma^2_{\mathcal{L}}U_{\rm ns}} \sim 0.5 \quad \text{for } T \approx 1.4 \text{ K},$$
$$U_{\rm ns} = 1 \text{ cm/s},\ H = 1 \text{ cm}. \tag{17d}$$

This means that the value $k_\times$, for which $\zeta(k_\times)=2$, is a few times larger than $k_{\min}\simeq \pi/H$. Therefore, for large scales (between H and $R_\times \simeq \pi/k_\times$), we expect significant coupling of the normal- and superfluid velocities: for $\zeta = 0.5$, Eq. (15b) gives $\mathcal{E}_{\rm ns}/\mathcal{E}^{(0)}_{\rm ns} \simeq 0.9$. The value of $\zeta_{\min}$ is inversely proportional to $U_{\rm ns}$ and, for $U_{\rm ns} > 1$ cm/s, becomes even smaller than 0.5. Accordingly, for $U_{\rm ns} > 1$ cm/s, the interval between H and $R_\times$ becomes larger and the coupling between the normal- and superfluid velocities at the largest scale H is even stronger: the ratio $\mathcal{E}_{\rm ns}/\mathcal{E}^{(0)}_{\rm ns} > 0.9$.

IV. SUMMARY AND DISCUSSION

We demonstrated that the cross-correlation function between normal- and superfluid velocity fluctuations $\mathcal{E}_{\rm ns}(k)$ in a turbulent counterflow of ^{4}He is strongly affected by the relative velocity $U_{\rm ns}$. As described by Eqs. (14) and illustrated in Fig. 3, this effect is governed by a dimensionless decoupling parameter $\zeta(k) \propto k/U_{\rm ns}$, given by Eq. (17a). This parameter increases with k and, when $k \simeq k_{\max} \simeq \pi/\ell$, it reaches its maximum, $\zeta_{\max} \gg 1$, as estimated in Eq. (17b). Accordingly, the normal- and superfluid velocity fluctuations of small scales (i.e., for large wave numbers) are almost fully decoupled: the correlation $\mathcal{E}_{\rm ns}$ is much smaller than its value $\mathcal{E}^{(0)}_{\rm ns} \approx 1$ for $U_{\rm ns}=0$. On the contrary, at large scales, the energy-containing fluctuations of $R \sim H$ are almost fully coupled: $\mathcal{E}^{(0)}_{\rm ns} - \mathcal{E}_{\rm ns} \ll \mathcal{E}^{(0)}_{\rm ns}$. The crossover scale $R_\times$, for which $\mathcal{E}_{\rm ns} = \frac{1}{2}\,\mathcal{E}^{(0)}_{\rm ns}$, is a few times smaller than H. Therefore, the large-scale fluctuations, for $H \gtrsim R \gtrsim R_\times$, may be qualitatively considered as coupled: $\mathcal{E}_{\rm ns} \geq \frac{1}{2}\mathcal{E}^{(0)}_{\rm ns}$. On the other hand, in the large interval of small scales, for $R_\times \gtrsim R \gtrsim \ell$ the normal- and superfluid velocities may be considered as effectively decoupled: $\mathcal{E}_{\rm ns} \leq \frac{1}{2}\mathcal{E}^{(0)}_{\rm ns}$.

The coupling or decoupling of normal- and superfluid velocities crucially affects the energy dissipation due to the mutual friction. Correspondingly, it also affects the energy spectra $\mathcal{E}_{\rm s}(k,t)$ and $\mathcal{E}_{\rm n}(k,t)$. To see this, let us consider the evolution equations for these objects, which may be obtained by multiplying Eqs. (3a) and (3b) in $(\boldsymbol{k},t)$ representation by $\boldsymbol{v}_{\rm s}(\boldsymbol{k},t)$ and $\boldsymbol{v}_{\rm n}(\boldsymbol{k},t)$, respectively, and averaging with respect to the turbulent statistics and directions of $\boldsymbol{k}$:

$$\left[\frac{\partial}{2\,\partial t} + k^2\nu'_{\rm s}\right]\mathcal{E}_{\rm s}(k,t) + \mathcal{NL}_{\rm s} = \Omega_{\rm s}[\mathcal{E}_{\rm ns}(k,t) - \mathcal{E}_{\rm s}(k,t)], \tag{18a}$$

$$\left[\frac{\partial}{2\,\partial t} + k^2\nu_{\rm n}\right]\mathcal{E}_{\rm n}(k,t) + \mathcal{NL}_{\rm n} = \Omega_{\rm n}[\mathcal{E}_{\rm ns}(k,t) - \mathcal{E}_{\rm n}(k,t)]. \tag{18b}$$

Here, $\mathcal{NL}_{\rm s,n}$ are nonlinear terms. For $k \gg k_\times$, due to the decoupling, $\mathcal{E}_{\rm ns}(k) \ll \mathcal{E}_{\rm s}(k)$. Therefore, it may be neglected on the right-hand side of Eq. (18a), which becomes $-\Omega_{\rm s}\mathcal{E}_{\rm s}$. This is similar to the equation for $\mathcal{E}_{\rm s}$ for superfluid turbulence in ^{3}He, where mutual friction drastically suppresses the energy spectrum $\mathcal{E}_{\rm s}(k)$ [10,18,27]; instead of the classical Kolmogorov spectrum $\mathcal{E}(k) \propto k^{-5/3}$, one finds the spectrum discussed by Lvov *et al.* [18]:

$$\mathcal{E}_{\rm s}(k) \propto \frac{1}{k^{5/3}}\left[\frac{1}{k^{2/3}} - \frac{1}{k_*^{2/3}}\right]^2, \tag{19}$$

which terminates at some critical value k_*. This means that provided that there exists a full decoupling of the velocities, the situation in the counterflowing superfluid component of ^{4}He becomes similar to that in ^{3}He turbulence with a normal-fluid component at rest. Thus one expects that the spectrum (19) describes the energy distribution between scales for $k \gg k_\times$.

For $k < k_\times$, due to the partial velocity correlations, the energy dissipation is much weaker than for $k > k_\times$, although it cannot be neglected as in coflowing ^{4}He, with classical Kolmogorov-1941 (K41) energy spectrum. Thus we can expect only moderate suppression of the energy spectrum as compared to the K41 case, as was recently observed in Ref. [28].

A more detailed analysis of the energy spectra $\mathcal{E}_{\rm s}(k)$ and $\mathcal{E}_{\rm n}(k)$ in the counterflowing ^{4}He that account for the decoupling of the normal- and superfluid turbulent velocity fluctuations and the resulting energy dissipation due to the mutual friction is beyond the scope of this paper.

ACKNOWLEDGMENTS

We acknowledge L. Skrbek, S. Babuin, and E. Varga for numerous and useful discussions of the similarities and differences between co- and counterflowing turbulence of superfluid ^{4}He, which inspired the current research. V.S.L. and A.P. acknowledge the kind hospitality while at Prague University and the support of EuHIT project "V-Front" that made their visit possible.

APPENDIX: SOME DEFINITIONS AND KNOWN RELATIONSHIPS

To find the cross correlation $\langle \boldsymbol{u}'_{\rm n}\cdot\boldsymbol{u}'_{\rm s}\rangle$, we need to recall some definitions and relationships required for our derivation, which are well-known in statistical physics. The first is the set of Fourier transforms in the following normalization:

$$\boldsymbol{u}'_{\rm n,s}(\boldsymbol{r},t) \equiv \int \frac{d\boldsymbol{k}}{(2\pi)^3}\,\boldsymbol{v}_{\rm n,s}(\boldsymbol{k},t)\exp(i\boldsymbol{k}\cdot\boldsymbol{r}), \tag{A1a}$$

$$\boldsymbol{v}_{\rm n,s}(\boldsymbol{k},t) \equiv \int \frac{d\omega}{2\pi}\,\widetilde{\boldsymbol{v}}_{\rm n,s}(\boldsymbol{k},\omega)\exp(-i\omega t), \tag{A1b}$$

$$\widetilde{\boldsymbol{v}}_{\rm n,s}(\boldsymbol{k},\omega) = \int d\boldsymbol{r}dt\,\boldsymbol{u}'_{\rm n,s}(\boldsymbol{r},t)\exp[i(\omega t - \boldsymbol{k}\cdot\boldsymbol{r})]. \tag{A1c}$$

The same normalization will be used for other objects of interest.

Next we define the simultaneous correlations and cross correlations in $\boldsymbol{k}$ representation (proportional to $\delta(\boldsymbol{k}-\boldsymbol{k}')$ due to homogeneity),

$$\langle \boldsymbol{v}_{\rm n}(\boldsymbol{k},t)\cdot\boldsymbol{v}^*_{\rm n}(\boldsymbol{k}',t)\rangle = (2\pi)^3 E_{\rm nn}(\boldsymbol{k})\,\delta(\boldsymbol{k}-\boldsymbol{k}'), \tag{A2a}$$

$$\langle \boldsymbol{v}_{\rm s}(\boldsymbol{k},t)\cdot\boldsymbol{v}^*_{\rm s}(\boldsymbol{k}',t)\rangle = (2\pi)^3 E_{\rm ss}(\boldsymbol{k})\,\delta(\boldsymbol{k}-\boldsymbol{k}'), \tag{A2b}$$

$$\langle \boldsymbol{v}_{\rm n}(\boldsymbol{k},t)\cdot\boldsymbol{v}^*_{\rm s}(\boldsymbol{k}',t)\rangle = (2\pi)^3 E_{\rm ns}(\boldsymbol{k})\,\delta(\boldsymbol{k}-\boldsymbol{k}'). \tag{A2c}$$

We also need to define cross correlations $\langle \widetilde{\boldsymbol{v}}_{\rm n}\cdot\widetilde{\boldsymbol{v}}^*_{\rm s}\rangle$ in $(\boldsymbol{k},\omega)$ representation,

$$\langle \widetilde{\boldsymbol{v}}_{\rm n}(\boldsymbol{k},\omega)\cdot\widetilde{\boldsymbol{v}}^*_{\rm s}(\boldsymbol{k}',\omega')\rangle = (2\pi)^4\widetilde{E}_{\rm ns}(\boldsymbol{k},\omega)\,\delta(\boldsymbol{k}-\boldsymbol{k}')\,\delta(\omega-\omega'). \tag{A3a}$$

This object is related to the simultaneous $\langle \boldsymbol{v}_n \cdot \boldsymbol{v}_s^* \rangle$ cross correlation (A2c) via the frequency integral,

$$\langle \boldsymbol{v}_n(\boldsymbol{k},t) \cdot \boldsymbol{v}_s^*(\boldsymbol{k}',t) \rangle = \int d\omega \widetilde{E}_{ns}(\boldsymbol{k},\omega). \tag{A3b}$$

Here and below, the tilde marks the objects defined in $(\boldsymbol{k},\omega)$ representation.

It is known also that the $\boldsymbol{k}$ integration of the correlations (A2) produces their one-point second moment:

$$\int \frac{d\boldsymbol{k}}{(2\pi)^3} E_{nn}(\boldsymbol{k}) = \langle |\boldsymbol{u}_n(\boldsymbol{r},t)|^2 \rangle, \tag{A4a}$$

$$\int \frac{d\boldsymbol{k}}{(2\pi)^3} E_{ss}(\boldsymbol{k}) = \langle |\boldsymbol{u}_s(\boldsymbol{r},t)|^2 \rangle, \tag{A4b}$$

$$\int \frac{d\boldsymbol{k}}{(2\pi)^3} E_{ns}(\boldsymbol{k}) = \langle \boldsymbol{u}_n(\boldsymbol{r},t) \cdot \boldsymbol{u}_s(\boldsymbol{r},t) \rangle. \tag{A4c}$$

In the isotropic case, each of the three correlations $E_{\dots}(\boldsymbol{k})$ is independent of the direction of $\boldsymbol{k}$: $E_{\dots}(\boldsymbol{k}) = E_{\dots}(k)$ and $\int \dots d\boldsymbol{k} = 4\pi \int \dots k^2\, dk$. This allows the introduction of the one-dimensional energy spectra $\mathcal{E}_s, \mathcal{E}_n$ and the cross correlation $\mathcal{E}_{ns}$ as follows:

$$\mathcal{E}_n(k) = \frac{k^2}{2\pi^2} E_{nn}(k), \quad \mathcal{E}_s(k) = \frac{k^2}{2\pi^2} E_{ss}(k),$$
$$\mathcal{E}_{ns}(k) \equiv \frac{k^2}{2\pi^2} E_{ns}(k). \tag{A5}$$

[1] R. J. Donnelly, *Quantized Vortices in Helium II* (Cambridge University Press, Cambridge, 1991).
[2] *Quantized Vortex Dynamics and Superfluid Turbulence*, edited by C. F. Barenghi, R. J. Donnelly, and W. F. Vinen, Lecture Notes in Physics, Vol. 571 (Springer-Verlag, Berlin, 2001)
[3] L. Skrbek and K. R. Sreenivasan, Phys. Fluids **24**, 011301 (2012).
[4] C. F. Barenghi, V. S. L'vov, and P.-E. Roche, Proc. Natl. Acad. Sci. USA **111**, 4683 (2014).
[5] M. R. Smith, R. J. Donnelly, N. Goldenfeld, and W. F. Vinen, Phys. Rev. Lett. **71**, 2583 (1993).
[6] P. L. Walstrom, J. G. Weisend, J. R. Maddocks, and S. W. Van Sciver, Criogenics **28**, 101 (1988).
[7] S. Babuin, E. Varga, and L. Skrbek, J. Low Temp. Phys. **175**, 324 (2014).
[8] H. E. Hall and W. F. Vinen, Proc. R. Soc. A **238**, 204 (1956).
[9] K. W. Schwarz and J. R. Rozen, Phys. Rev. Lett. **66**, 1898 (1991).
[10] V. S. L'vov, S. V. Nazarenko, and L. Skrbek, J. Low Temp. Phys. **145**, 125 (2006).
[11] P.-E. Roche, C. F. Barenghi, and E. Leveque, Europhys. Lett. **87**, 54006 (2009).
[12] J. Tchoufag and P. Sagaut, Phys. Fluids **22**, 125103 (2010).
[13] L. Boué, V S. L'vov, Y. Nagar, S. V. Nazarenko, A. Pomyalov, and I. Procaccia, Phys. Rev. B **91**, 144501 (2015).
[14] L. Boué, V. S. L'vov, A. Pomyalov, and I. Procaccia, Phys. Rev. Lett. **110**, 014502 (2013).
[15] W. F. Vinen, J. Low Temp. Phys. **175**, 305 (2014).
[16] I. L. Bekarevich and I. M. Khalatnikov, Sov. Phys. JETP **13**, 643 (1961).
[17] W. F. Vinen and J. J. Niemela, J. Low Temp. Phys. **128**, 167 (2002)
[18] V. S. L'vov, S. V. Nazarenko, and G. E. Volovik, JETP Lett. **80**, 479 (2004).
[19] K. W. Schwarz, Phys. Rev. B **38**, 2398 (1988).
[20] L. Kondaurova, V. S. L'vov, A. Pomyalov, and I. Procaccia, Phys. Rev. B **90**, 094501 (2014)
[21] R. H. Kraichnan, J. Fluid Mech. **5**, 497 (1959).
[22] H. W. Wyld, Ann. Phys. (NY) **14**, 143 (1961).
[23] V. S. L'vov, Yu. L'vov, A. C. Newell, and V. E. Zakharov, Phys. Rev. E **56**, 390 (1997).
[24] V. S. L'vov and I. Procaccia, Phys. Rev. E **52**, 3840 (1995); **52**, 3858 (1995).
[25] L. Kondaurova, V. S. L'vov, A. Pomyalov, and I. Procaccia, Phys. Rev. B **89**, 014502 (2014).
[26] R. J. Donnelly and C. F. Barenghi, J. Phys. Chem. Ref. Data **27**, 1217 (1998)
[27] L. Boué, V. S. L'vov, A. Pomyalov, and I. Procaccia, Phys. Rev. B **85**, 104502 (2012)
[28] A. Marakov, J. Gao, W. Guo, S. W. Van Sciver, G. G. Ihas, D. N. McKinsey, and W. F. Vinen, Phys. Rev. B **91**, 094503 (2015).